G 4/4

Influence Functions for Surface Flaws in Pressure Vessels

P.P. Milella
ENEA, Via Brancati 48, I-00100 Roma, Italy
C. Sampietri
CISE S.p.A., C.P. 12081, I-20134 Milano, Italy

Abstract

The aim of this paper is to determine the influence function distributions around the crack front for longitudinal semi-elliptical surface flaws in the beltline region and for a partly circular or elliptical crack in the nozzle shell course region of a PWR vessel.
As far as the cylinder is concerned, the following crack geometries are considered: $a/c=1/3$, $1/2$, $R_i/t=10$, $a/t=0.1,0.2,0.4,0.6$; where a is the semi-minor axis of the ellipse, c is the semi-major axis, R_i is the inside radius of the cylinder and t is its thickness.
Four separate loadings for each crack geometry are considered.
In the nozzle region the cracks are characterized by the following ratios: $a/c=1.0$, $a/t=0.2$, 0.3, 0.5, 0.7 and $a/c=1/2$, $a/t=0.15$, 0.2, 0.3, 0.45.
In this case, seven loads are considered.

Finally, the influence functions are compared with those by other authors.

1. Introduction

The linear elastic fracture mechanics is at present extensively used in the design of nuclear power plants.
Its application, according to the ASME pressure vessel code, requires the computation of stress intensity factor K for some typical flaws. The evaluation of K around the crack front for elliptical or circular surface flaws, occurring in some critical regions of the nuclear vessel and subjected to particular loading conditions, is very interesting.
These regions are usually located at the nozzles, where strong geometrical variations cause high stress concentrations, and at the beltline, near the core, where nuclear radiations, induce degradation in the material properties. Among the current techniques, the finite element method turns out to be particularly effective to evaluate the K factor but these calculations, usually in three dimensions, are a heavy computational task. This drawback may be considerably simplified if influence function libraries are available. The calculation of influence functions for some typical geometries is the purpose of this paper.

2. Influence functions for semi-elliptical cracks in cylinders

The influence functions concerning four simple loading types were determined for longitudinal semi-elliptical cracks which are on the internal surface of a cylinder. The results, quoted in /1/, refer to different shapes relevant to the geometrical ratios (fig.1): $a/c=1/3$

and 1/2, a/t=0.1, 0.2, 0.4, 0.6: $R_i/t=10$ where a is the semi-minor axis of the ellipse, c is the semi-major axis, t is the thickness of the cylinder and R_i is the inside radius. On the basis of the particular symmetry of the structure, only a quarter of the whole cylinder was considered by applying the suitable constraints of symmetry. No constraint was imposed on the axial direction. For the finite element idealization of the structure, 627 isoparametric parabolic elements were used for a total of 3295 nodes. Every longitudinal section consisted of 33 elements and the subdivisions along the circumference of the cylinder were 19.
Every crack was subjected to four different loading types:

$$\sigma_0, \sigma_1\frac{x}{t}, \sigma_2\frac{x^2}{t^2}, \sigma_3\frac{x^3}{t^3} \tag{1}$$

The energy release rate for each load, G_i, was calculated along the crack front using the finite element computer-code TRISMEF /2/, based on the Parks method /3/. The corresponding stress intensity factor, K_i, was obtained by the following equation:

$$K_i = \sqrt{\frac{G_i E}{1-\nu^2}} \tag{2}$$

where E is the elastic modulus and ν is the Poisson's ratio.

Finally the influence function for each load was obtained by applying the following equation, see Liebowitz /4/:

$$H_i(\emptyset) = f_i \frac{K_i(\emptyset)}{\sqrt{\pi a}\,\sigma_i\left(\frac{a}{t}\right)^i} \quad \frac{E(K)}{\left(\cos^2\emptyset + \frac{a^2}{c^2}\sin^2\emptyset\right)^{1/4}} \tag{3}$$

$$f_0=1,\ f_1=\pi/2,\ f_2=2,\ f_3=3\pi/4 \tag{4}$$

where E(K) is the elliptical integral and all other symbols are defined in fig.1.

Some of the obtained results are shown in figs. 2 - 5.

The comparison of functions $H_i(\emptyset)$, obtained with the same loading type and ratio a/c, but with different ratio a/t, shows that the functions increase for increasing values of a. Only function $H_0(\emptyset)$, both for a/c=1/3 and a/c=1/2, shows a strong change if a/t=0.2 or a/t=0.4 is considered. In fact, when a/c=0.2, the function shows a maximum whereas, when a/c=0.4, it increases monotonically. On the contrary, the comparison between functions $H_i(\emptyset)$, obtained with the same loading type and ratio a/t but with different ratio a/c, shows that the values of $H_i(\emptyset)$ when a/c=1/3 are greater than those relevant to a/c=1/2. However, it can be noticed that the difference between the functions decreases when $\emptyset$ goes from 0° to 90°. Moreover, when is near 90°, the values of $H_i(\emptyset)$, computed for a/c=1/2, are generally greater than those relevant to a/c=1/3. This behaviour is present also in the results obtained by Heliot et al. /5/ even if they used different values of a/c.

The obtained results can be compared with those given by other authors through interpolation or extrapolation. In fact, Mc Gowan and Raymund /6/ have investigated the problem described in this paper, with the only difference that they have used a/t=0.25, 0.5, 0.8 and a/c=1/3. The same geometries were also studied by Heliot et al. /7/ using the B.I.E. method. Some comparisons are shown in fig.6. The proposed results show a better agreement with the results given by Mc Gowan and Raymund than with those given by Heliot et al.

3. Influence functions for circular and elliptical cracks in the nozzle corner

The influence functions concerning seven simple loading types for circular and elliptical cracks, which are in the nozzle corner of a PWR vessel, were calculated and the results are quoted in /8/. The dimensions of the considered geometry are shown in fig.7. The investigated cracks were characterized by the following geometrical ratios: a/c=1/2 (elliptical cracks), a/t=0.15,0.2,0.3, 0.45 where t is the thickness of the joint region, a is the semi-minor axis of the ellipse, c is the semi-major axis (parallel to the vessel axis) and a/c=1.0 (i.e. circular cracks), a/t=0.2, 0.3, 0.5, 0.7.

Every crack was subjected to seven different loading types:

$$\sigma_{00},\ \sigma_{10}\frac{x}{t},\ \sigma_{01}\frac{y}{t},\ \sigma_{20}\frac{x^2}{t^2},\ \sigma_{02}\frac{y^2}{t^2},\ \sigma_{30}\frac{x^3}{t^3},\ \sigma_{03}\frac{y^3}{t^3} \tag{5}$$

The influence function concerning each loading type was defined by the following equations /4/:

$$h_{io}(\phi)=\frac{K_{io}(\phi)}{\sigma_{io}\left(\frac{c}{t}\right)^{i}\sqrt{\pi a}}\ \frac{E(k)}{\left(\sin^2\phi+\frac{a^2}{c^2}\cos^2\phi\right)^{1/4}}\ ;$$

$$h_{oj}(\phi)=\frac{K_{oj}(\phi)}{\sigma_{oj}\left(\frac{a}{t}\right)^{j}\sqrt{\pi a}}\ \frac{E(k)}{\left(\sin^2\phi+\frac{a^2}{c^2}\cos^2\phi\right)^{1/4}} \tag{6}$$

where the stress intensity factors, K_{io} and K_{oj}, were obtained as in the previous case.

For the sake of brevity only some results are plotted in figs. 8 - 14. As an example of application, the influence functions are used to calculate the stress intensity factor,K, for an internally pressurized cylinder. The stress intensity factor, obtained as above and averaged along the crack front, was then normalized in the following way, proposed by Mohamed and Schroeder /9/:

$$F' = \frac{\frac{K}{\sigma\sqrt{\pi d}}}{1+\left(\frac{rt}{RT}\right)^{1/2}} \tag{7}$$

where d is the crack depth, σ is the hoop stress, r and t are the radius and thickness of the nozzle, and R and T are the radius and thickness of the cylinder.

Fig. 15 summarizes the comparison with the results obtained by Rashid and Gilman /10/, Broekhoven and Van de Ruijtenbeek/11/, Broekhoven/12/, Besuner et al. /13/, Heliot et al. /14/.

The agreement, usually good, becomes better in case of deeper cracks.

4. Conclusions

The influence functions were determined by means of a three-dimensional finite element computer-code for some cracks having various shapes and located in the critical regions of a nuclear vessel. As far as the cracks in the beltline region are concerned, the proposed functions are slightly underestimated even if they show a trend similar to that referred to in the literature. The difference, usually small, decreases with the increase of the crack depth.

The stress intensity factors, computed by means of the influence functions for the cracks in the nozzle corner, are in good agreement with those obtained by other authors. Minor differences could be due to small differences in the geometries considered by the above mentioned authors.

BIBLIOGRAPHY

/ 1 / E. Meregalli, C. Sampietri, "Calcolo dei coefficienti di influenza per cricche longitudinali semiellittiche in un cilindro", CISE 2219 (1983)

/ 2 / A. Cella, A. Greco, C. Lusso, "Meccanica della frattura lineare elastica: TRISMEF, un programma di calcolo tridimensionale statico per il calcolo della grandezza G", CISE 2056 (1983)

/ 3 / D.M. Parks, "A StiffnessDerivative Finite Element Technique for Determination of Crack Tip Stress Intensity Factors", International Journal of Fracture (1974)

/ 4 / M. Liebowitz, "Fracture", Academic Press (1968)

/ 5 / J. Heliot, R.C. Labbens, A. Pellissier-Tanon, "Solution of Three Dimensional Crack Problem Using the Boundary Integral Equation Method", Numerical Methods in Fracture Mechanics (1980)

/ 6 / J.J. Mc Gowan, M. Raymund, " Stress Intensity Factor Solutions for Internal Longitudinal Semi-Elliptical Surface Flaws in a Cylinder Under Arbitrary Loadings", Fracture Mechanics ASTM STP 677 (1979)

/ 7 / J. Heliot, R.C. Labbens, A. Pellisier - Tanon, "Semi-Elliptical Cracks in a Cylinder Subjected to Stress Gradient", (1978)

/ 8 / C. Sampietri, "Calcolo dei coefficienti di influenza per cricche d'angolo nella regione del bocchello di un recipiente PWR", CISE 2431 (1984)

/ 9 / M.A. Mohamed, J. Schroeder, "Stress Intensity Factor Solution for Crotch- Corner Cracks of Tee - Intersections of Cylindrical Shell", International Journal of Fracture (1978)

/10 / Y.R. Rashid, J.D. Gilman, "Three Dimensional Analysis of Reactor Pressure Vessel Nozzles", First International Conference on Structural Mechanics in Reactor Technology, Paper G2/6 (1971)

/11 / M. Broekhoven, M. Van de Ruitenbeek, "Fatigue Crack Extension in Nozzle Junctions; Comparison of Analytical Approximations with Experimental Data", Third International Conference on Structural Mechanics in Reactor Technology, Paper G4/7 (1975)

/ 12 / M. Broekhoven, "Computation of Stress Intensity Factors for Nozzle Corner Cracks by Various Finite Element Procedures", Third International Conference on Structural Mechanics in Reactor Technology, Paper G4/6 (1975)

/ 13 / P.M.Besuner , L.M. Cohen, J.L. Mc Lean, "The Effects of Location, Thermal Stress, and Residual Stress on Corner Cracks in Nozzles with Cladding", Fourth International Conference on Structural Mechanics in Reactor Technology, Paper G4/5 (1977)

/ 14 / J. Heliot, R. Labbens, F. Robisson, "Influence Functions for Stress Intensity Factors at a Nozzle Corner", ASTM STP 743 (1981)

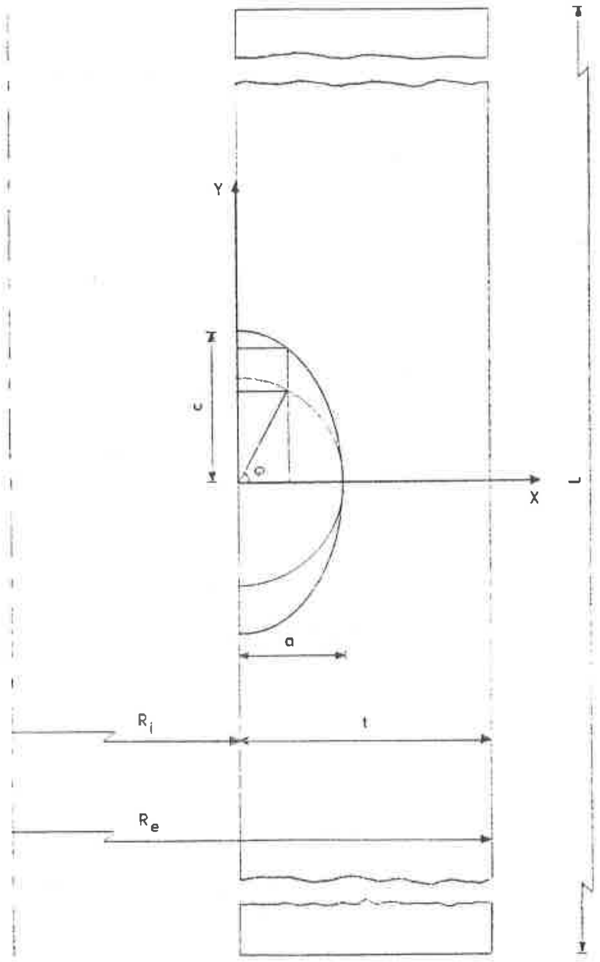

R_i = 1997 mm
R_e = 2197 mm
L = 3200 mm

Fig. 1 - Semi-elliptical crack in a cylinder

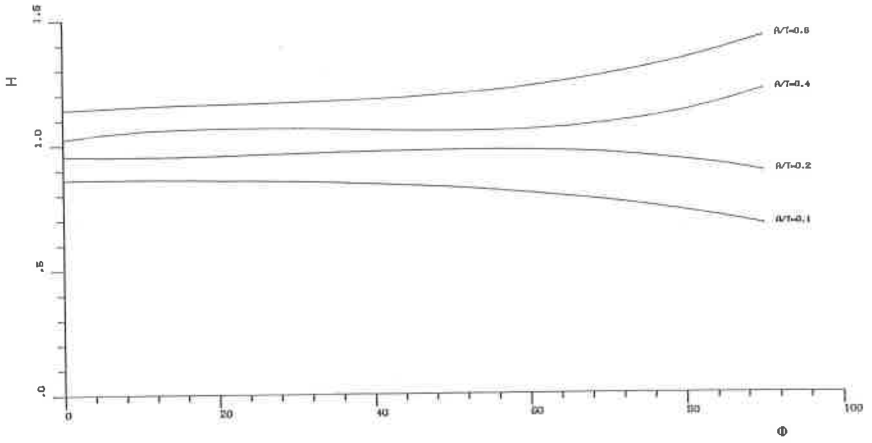

Fig. 2 - Influence functions H_0 (a/c=1/2)

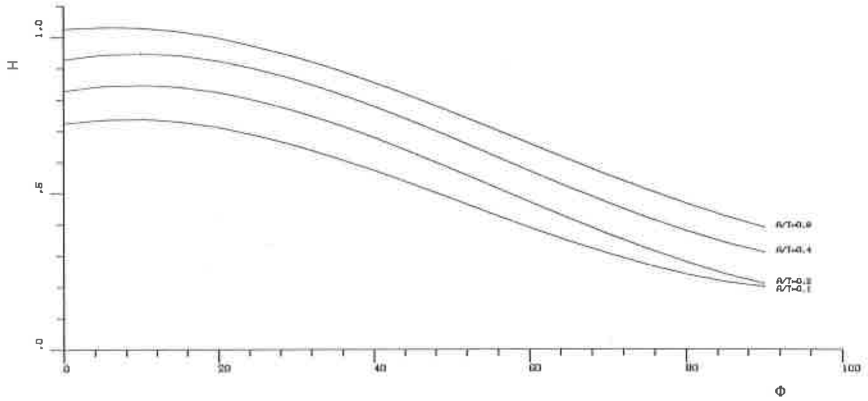

Fig. 3 - Influence functions H_1 'a/c=1/2)

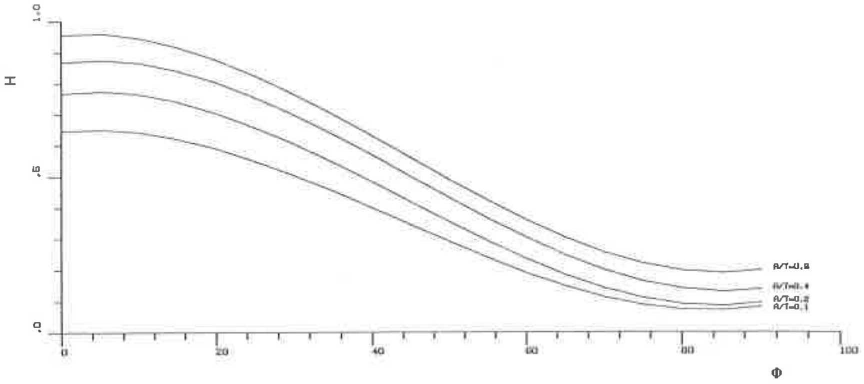

Fig. 4 - Influence functions H_2 (a/c=1/2)

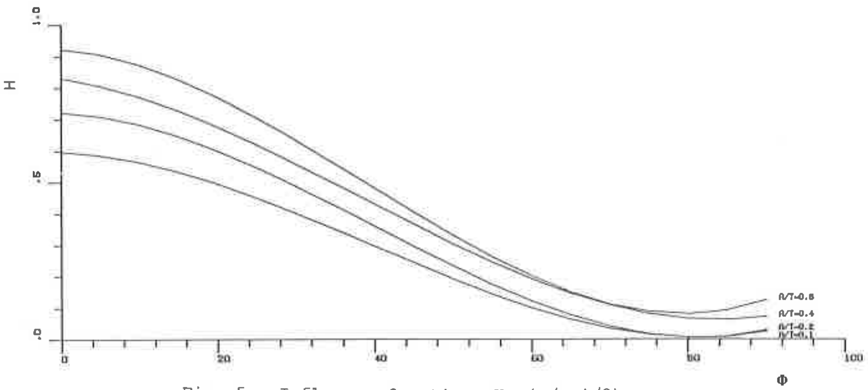

Fig. 5 - Influence functions H_3 (a/c=1/2)

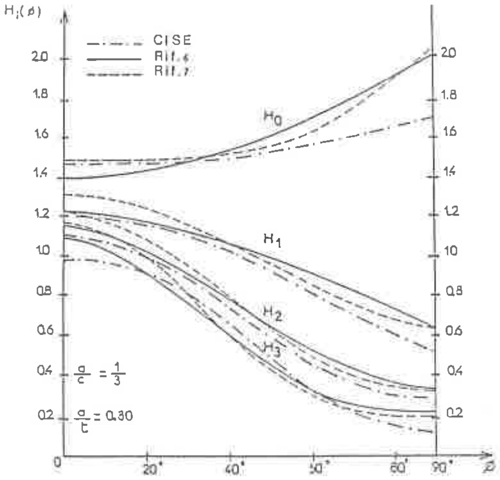

Fig. 6 - Crack in cylinder: comparison with other authors

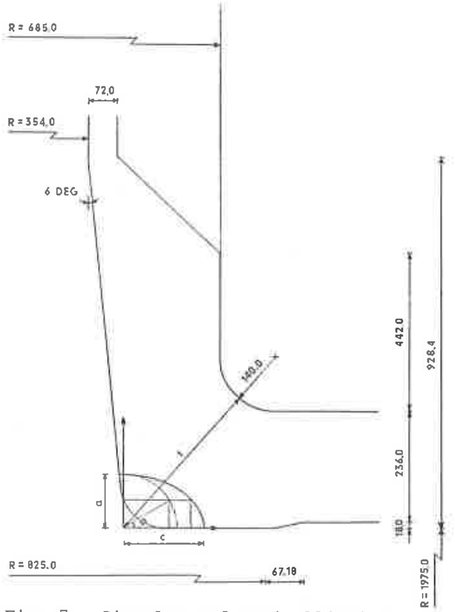

Fig. 7 - Circular and semi-elliptical cracks at a nozzle corner

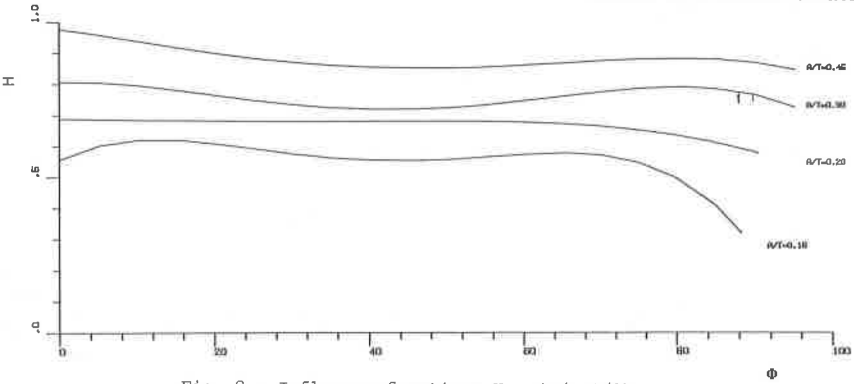

Fig. 8 - Influence functions H_{00} (a/c=1/2)

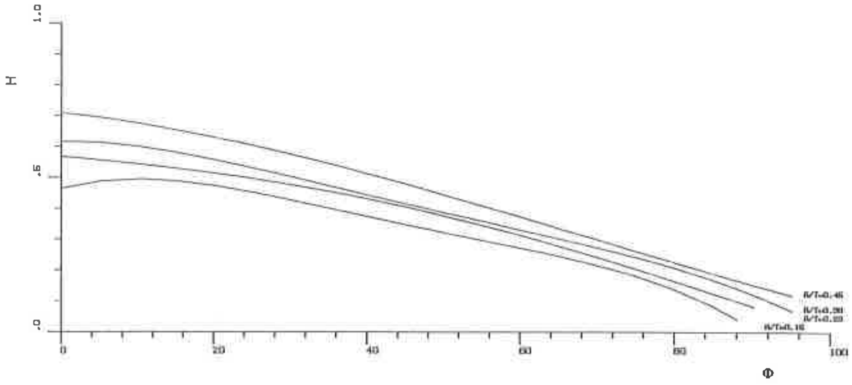

Fig. 9 - Influence functions H_{10} (a/c=1/2)

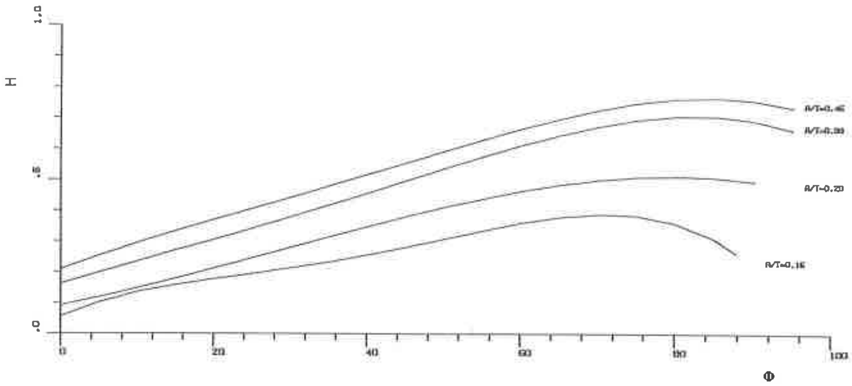

Fig.10 - Influence functions H_{01} (a/c=1/2)

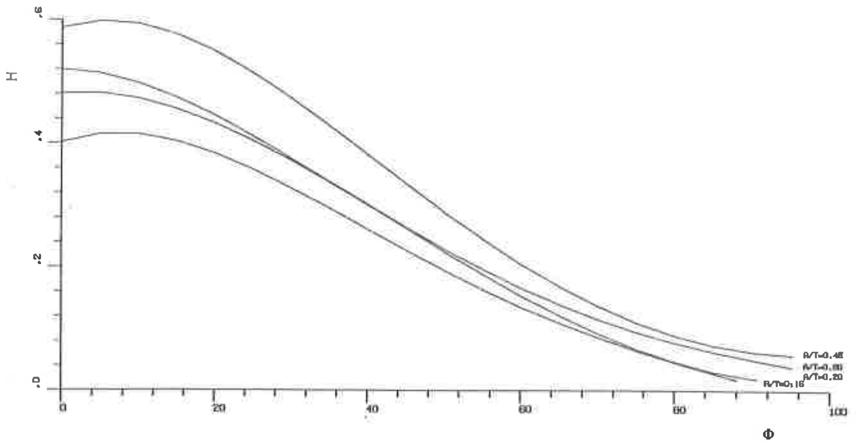

Fig.11 - Influence functions H_{20} (a/c=1/2)

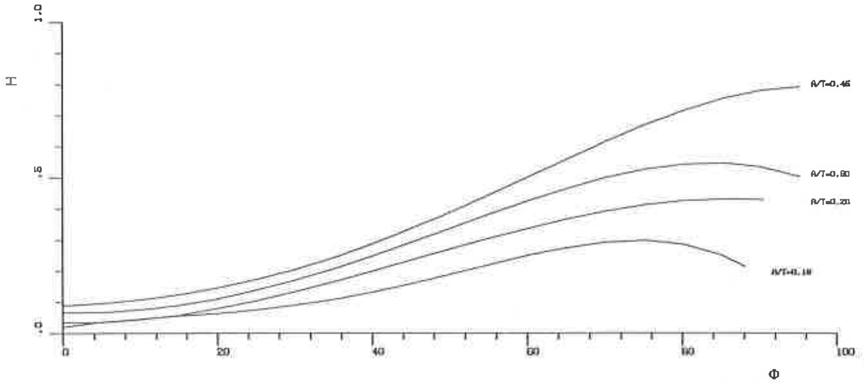

Fig.12 - Influence functions H_{02} (a/c=1/2)

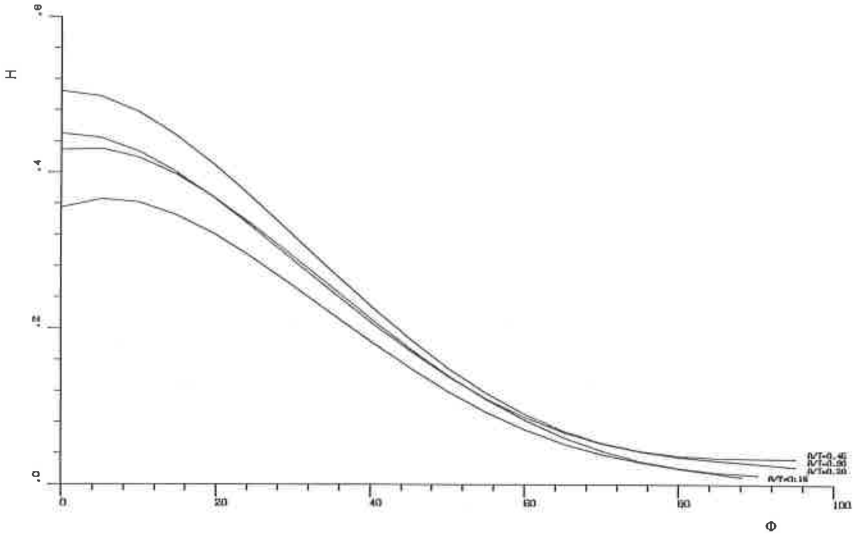

Fig.13 - Influence functions H_{30} (a/c=1/2)

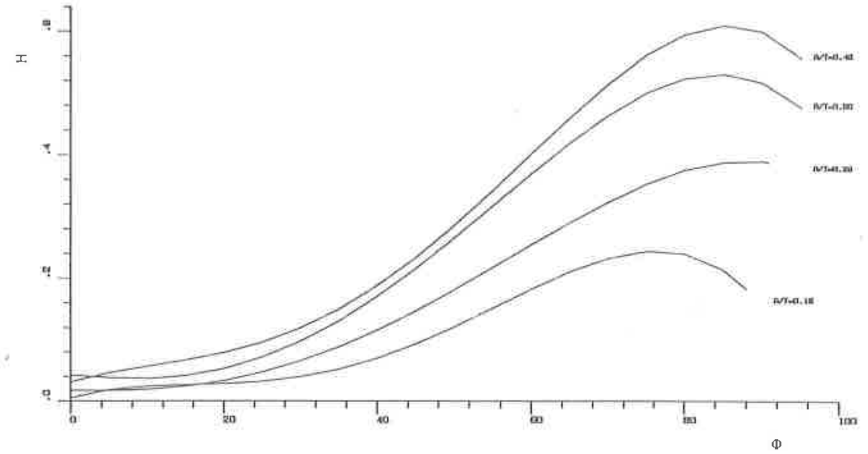

Fig.14 - Influence functions H_{03} (a/c=1/2)

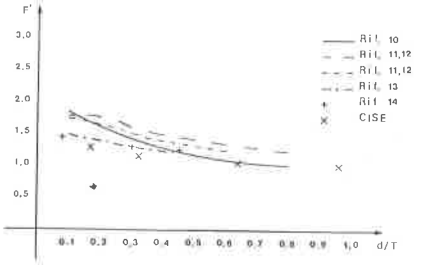

Fig.15 - Crack at nozzle corner: comparison with other authors